  Bull. Chem. Soc. Jpn., 55, 699—703 (1982)

Preparation and Physical Properties of EuC_2 and Its Solid Solutions, $R_xEu_{1-x}C_2$ (R=La and Gd)

Tetsuo SAKAI, Gin-ya ADACHI,* Takeshi YOSHIDA, Shin-ya UENO, and Jiro SHIOKAWA

Department of Applied Chemistry, Faculty of Engineering, Osaka University, Yamadaoka 2-1, Suita, Osaka 565

(Received August 10, 1981)

A cubic-tetragonal phase transformation of EuC_2 was observed at 623 K. The phase transition temperatures of metal dicarbides (MC_2) were discussed in terms of the band structure proposed by previous authors. The compound EuC_2 was a ferromagnet with a zero field curie temperature of 20 K, which was close to the value expected from the Curie temperature *vs.* nearest neighbor Eu–Eu distance relation for the Eu chalcogenides. The solid solutions, $La_xEu_{1-x}C_2$, became ferromagnetic at low temperatures over the whole composition range, while the solid solutions, $Gd_xEu_{1-x}C_2$, have continuously changed the kind of magnetic order from ferromagnetic to antiferromagnetic. All the effective moments obtained for $R_xEu_{1-x}C_2$ were in good agreement with the theoretical values of Eu^{2+} and R^{3+} contained. The electrical resistivities of EuC_2 and its solid solutions had a sharp peak near the Curie temperature. When magnetic field was applied, the peak became broader and shifted to higher temperature.

Metal dicarbides (MC_2), which possess a CaC_2-type tetragonal structure at room temperature, are composed of metal ion (M^{n+}), acetylide ion (C_2^{2-}), and $(n-2)$ electrons. Since the $(n-2)$ electrons occupy a conduction band,[1] tervalent or quadrivalent metals form metallic dicarbides, while bivalent metals form nonmetallic dicarbides. An isostructural europium dicarbide (EuC_2), whose existence has been established by Gebelt and Eick,[2] is expected to contain bivalent europium ions (Eu^{2+}) and has a variety of interesting physical properties such as observed for Eu chalcogenides.[3] However, in contrast with the tervalent rare-earth dicarbides which have been intensively investigated, the carbide EuC_2 has received the least attention to date. In this paper, we report thermal, magnetic, and electrical properties of EuC_2 and its solid solutions, $R_xEu_{1-x}C_2$ (R=La and Gd).

Experimental

Europium carbide was synthesized by following two techniques. (1) Europium metal of 99% purity (Research Chemicals, Div. of Nucor Corp.) together with spectroscopic grade graphite (Nippon Carbon Corp.) was sealed under a vacuum (10^{-2} Pa) in a silica capsule and heated at 1000 °C for 30 h. (2) Europium oxide of 99.99% (Shin-etsu Chem. Corp.) was mixed with graphite powder in an agate mortar and then pressed into pellets at 10 kbar. The pellets were placed in a molybdenum container and heated at 1800 °C under a flow of argon for 5 h. Solid solutions, $La_xEu_{1-x}C_2$ and $Gd_xEu_{1-x}C_2$, were prepared from mixed lanthanoid oxides and graphite by heating them under the same conditions as the above method (2). The mixed oxides as starting materials were obtained as follows; europium and gadolinium (or lanthanum) trioxides (99.99% purity) were weighed and dissolved in 2 mol dm^{-3} HCl and a saturated solution of oxalic acid was added. The precipitate formed was filtered, oven-dried at 110 °C, and ignited at 900 °C. Strontium dicarbide was synthesized by the reaction of $SrCO_3$ (99.9%, Shin-etsu Chem. Corp.) and graphite at 1600 °C under an argon atmosphere. In all cases, 5 at% excess graphite was used to ensure removal of oxides. The samples obtained here were kept immersed in carbon tetrachloride or in evacuated glass capsules. All manipulations were carried out in an argon dry box in order to prevent hydrolysis.

Powder X-ray diffraction data were obtained with a Rigaku-Denki Rota-flex diffractometer by use of Ni-filtered Cu $K\alpha$ radiation and Si as an internal standard. The atomic ratios (La or Gd:Eu) in the solid solutions were determined with a Rigaku-Denki energy dispersion type X-ray fluorescent spectrograph unit, Ultra trace system. For the purpose of chemical analyses, weighed sample was hydrolyzed in 2 mol dm^{-3} HCl. After the solution was filtered to remove the free graphite, metal content in it was determined by the EDTA titration. Total carbon content was determined by elemental analysis with a Yanagimoto CHN-corder. Bound carbon content was obtained by the difference between the total and free carbon contents. These analyses gave the weight percentages of the free carbon in the range of 1—2% and a metal:bound carbon atomic ratio of 1:2 for all the carbides.

Phase transformation was examined by the method reported previously;[4] differential thermal analysis (DTA) in the range 290—1000 K. Magnetic susceptibility data were obtained with a Curie-chénevea magnetic balance (Shimadzu MB-11) equipped with a low temperature apparatus in the temperature range 4.2—300 K. The samples for magnetic measurements were mixed with apiezon grease L (Apiezon Products Ltd.) to protect them from moist air. Electrical resistivities were measured with strip samples cut from the polycrystalline sintered pellets in the range 1.5—300 K. The measurements were performed on a four-probe d.c. potentiometric technique. Thermoelectric power measurement was carried out in the range 120—300 K. A barshaped sample was held in a place between two copper blocks with Ag paste. Thermal gradient was controlled by small heaters wound on the copper blocks so as to be always less than 5 K.

Results and Discussion

X-Ray Data. Both of the europium carbides obtained by the two different methods possess the CaC_2-type body-centered tetragonal structure though they contain a second phase. This second phase, whose existence has been reported by previous authors,[2] could not be removed by annealing techniques. The lattice constants of the b.c.t. phase are in good agreement with the literature values[2] and those obtained for SrC_2 as shown in Table 1. Since Sr^{2+} in SrC_2 has the almost same ionic radius as Eu^{2+},

this result supports the assumption that all the Eu ions in EuC_2 are bivalent.

Rare-earth dicarbides, LaC_2 and EuC_2, form solid solutions ($La_xEu_{1-x}C_2$) with the b.c.t. structure. The sample of $x=0.08$ contains the same unknown phase as observed for EuC_2, while the sample of the composition range from $x=0.39$ to 0.94 are single phase of b.c.t. The lattice constants of $La_xEu_{1-x}C_2$ are summarized in Table 2.

For the solid solutions, $Gd_xEu_{1-x}C_2$, the compounds with compositions of $x=0.13$, 0.73, and 0.92 are formed with the b.c.t phase, while the compounds of $x=0.40$ and 0.62 have a face-centered cubic structure. The occurrence of the f.c.c. phase has been observed by previous authors[5] in the binary systems RC_2–$R'C_2$ (R=rare-earth elements). This phenomenon has been explained successfully in terms of a strain energy in the crystal which was produced by a large difference in the ionic radii of metals.[6,7] The lattice parameters of $Gd_xEu_{1-x}C_2$ are tabulated in Table 3.

The disappearance of the unidentified second phase in the mixed carbides may be in connection with the increase of the conduction electron density.

Phase Transformation. It is well known that the CaC_2-type dicarbides have a transformation from the b.c.t. phase at low temperature to the f.c.c. one at high temperature. The nature of the cubic-tetragonal phase transformation has been studied extensively for metal dicarbides (MC_2) except for EuC_2.[4-14] The data of EuC_2 which we obtained are tabulated in Table 1, compared with those obtained for SrC_2. The f.c.c. modification in EuC_2 occurs at 623 K, which is close to the value observed for SrC_2.

The phase transition temperatures (T_t) of MC_2 vary significantly from 423 K for BaC_2[8] to 2058 K for UC_2.[9] Since the transformation in MC_2 occurs through rotation of the C_2^{2-} group from the c-axis, the T_t values are expected to reflect the M–C_2 bond energy and then depend on two parameters; ionic radius of metal and the number of the conduction electrons. We plotted the T_t values of MC_2 against the ionic radii of metals,[15] $r(M^{n+})$, for coordination number six in Fig. 1. The T_t values are divided into three groups with respect to the number of con-

Table 1. Lattice constants and phase transition temperatures of EuC_2 and SrC_2

	Ionic radius of M^{2+} a)	Lattice constants	Transition temperatures
	Å	Å	K
EuC_2	1.17	$a=4.118$	623±3
		$c=6.756$	
SrC_2	1.18	$a=4.103$	675±3
		$c=6.756$	(643) b)

a) Values reported in Ref. 15. b) Values reported in Ref. 8.

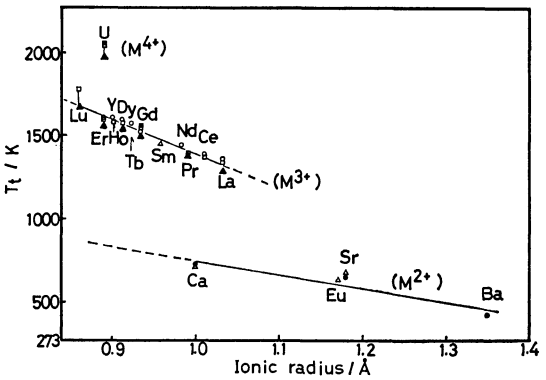

Fig. 1. Ionic radius of M^{n+} *vs.* phase transition temperature (T_t) plots for MC_2.
●: Bredig,[8] ■: Wallace *et al.*,[9] ▲: McColm *et al.*,[7,11] □: Bowman *et al.*,[10] ○: Adachi *et al.*,[13,14] △: this work.

Table 2. Lattice constants and magnetic properties of the solid solutions, $La_xEu_{1-x}C_2$

x	a/Å	c/Å	T_c/K	θ_p/K	μ_{eff}/μ_B	μ_{cal}/μ_B
0.00a)	4.118	6.756	20	+14	8.04	7.94
0.08a)	4.072	6.696	20	+12	8.15	7.64
0.39	4.022	6.664	19	+15	6.33	6.19
0.47	3.990	6.627	19	+15	5.88	5.76
0.68	3.974	6.613	14	+15	5.02	4.48
0.76	3.944	6.580	11	+2	4.08	3.93
0.94	3.939	6.570	<4	0	2.11	1.90

a) These samples contain the second phase.

Table 3. Lattice constants and magnetic properties of the solid solutions, $Gd_xEu_{1-x}C_2$

x	a/Å	c/Å	Phase	$T_{ord.}$/K	θ_p/K	μ_{eff}/μ_B	$\mu_{calord.}/\mu_B$
0.13	4.066	6.551	b. c. t.	20 Fa)	+20	7.94	7.94
0.40	5.835		f. c. c.	12 F	+8	8.05	7.93
0.62	5.813		f. c. c.	<4 AFb)	−13	7.88	7.92
0.73	3.780	6.306	b. c. t.	AF	−28	8.10	7.91
0.92	3.736	6.298	b. c. t.	33 AF	−43	8.06	7.90
1.00	3.722	6.295	b. c. t.	42 AF	−53	7.67	7.90

a) Ferromagnetic. b) Antiferromagnetic.

duction electrons and increase linearly with decreasing the ionic radius of metal, that is, with an increase in the lattice energy. The T_t *vs.* $r(M^{n+})$ plot for $M^{2+}C_2^{2-}$ indicates that EuC_2 is a member of the bivalent metal dicarbide group.

It has been proposed by Atoji[1] that excess electrons occupy the conduction band formed with the d-orbitals (d_{zx} and d_{yz}, z≡c-axis) of metal and the antibonding orbitals of C_2^{2-} and that the increase of conduction electron density causes to increase the C–C bond distance in MC_2. Since the C–C bond distances in MC_2 seem to be independent of the ionic radii of M^{n+},[16,17] their average values are listed in Table 4. Assuming that the C–C bond distances increase with increasing the M–C_2 covalent bond energy, we can expect that the increase in the T_t value has a linear relationship with the C–C bond distance. In order to discuss the T_t values under the same ionic radius of metal, the T_t values at $r(M^{n+})=0.89$ Å, which is identical with the ionic radius of U^{4+}, were estimated from the linear T_t *vs.* $r(M^{n+})$ plots in Fig. 1 and summarized in Table 4. The T_t values of MC_2 are plotted linearly against the C–C bond distances in Fig. 2 in support of the above assumption.

Magnetic Properties. Magnetization (σ) *vs.* temperature (T) curves for EuC_2 are shown at various fields in Fig. 3. Inset is the field dependence of magnetization at various temperatures. These magnetic data exhibit that EuC_2 becomes ferromagnetic at low temperature. Curie temperatures (T_c) at various fields (H) were determined by the method described in Ref. 18; extrapolation of σ^2 *vs.* T plot to $\sigma^2=0$. The zero field Curie temperature, $T_c(H\to 0)=20$ K, was obtained from the $T_c(H)$ *vs.* H plot in Fig. 6. Reciprocal magnetic susceptibility (χ_m^{-1}) *vs.* T plot obeys a Curie-Weiss law, giving an effective moment of

Table 4. Phase transition temperatures estimated at the ionic radius of $r(M^{n+})=0.89$ Å, average values of the C–C bond distances, and the number of conduction electrons, $(n-2)$ for MC_2

	Transition temperature K	C–C bond distance Å	$(n-2)$
$M^{2+}C_2$	850	1.191	0
$M^{3+}C_2$	1615	1.286	1
$M^{4+}C_2$	2038	1.340	2

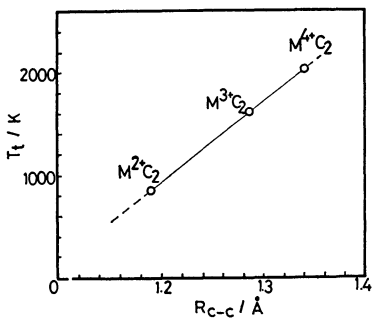

Fig. 2. Estimated phase transition temperature (T_t) *vs.* average C–C bond distance (R_{C-C}) plot for MC_2.

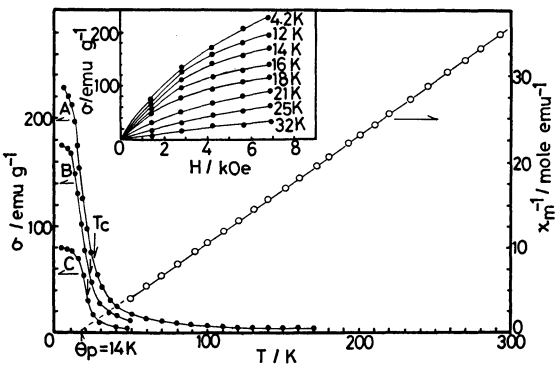

Fig. 3. Temperature dependence of magnetization (σ/emu g^{-1}†, —●—, A: 6.85 kOe††, B: 4.20 kOe, C: 1.40 kOe) and reciprocal magnetic susceptibility (χ_m^{-1}, —○—) for EuC_2.
† emu $g^{-1}=4\pi\times10^{-3}$ MKS kg^{-1}. †† 1 Oe=(1000/4π) A m^{-1}.

8.04 μ_B and a paramagnetic Curie temperature (θ_p) of +14 K. The effective moment is in good agreement with that expected for Eu^{2+}.

The exchange mechanism in EuX (X=O, S, and Se) has been studied by Kasuya.[19] They have proposed that the ferromagnetic interaction is due to the f-f interaction between Eu^{2+} nearest neighbors throughout the 5d-4f exchange interaction. Therefore, the exchange integral between Eu^{2+} nearest neighbours becomes a function of the Eu^{2+}–Eu^{2+} distance. The europium dicarbide has a nearest neighbour Eu^{2+} distance of 4.12 Å, which is very close to that of EuS, 4.21 Å. Since both the values of T_c and θ_p observed for EuC_2 are comparable to those of EuS ($T_c=16$ K, $\theta_p=19$ K), it is reasonable to assume that the exchange mechanism in EuC_2 is the same as that in EuX.

The tervalent rare-earth dicarbides (RC_2), which have one conduction electron per formulae unit, become antiferromagnetic at low temperatures.[20–22] Their magnetic properties have been discussed in terms of the f-f indirect exchange interaction *via* conduction electrons. The replacement of Eu^{2+} with La^{3+} varies two parameters, that is, the concentration of the conduction electron and the magnetic ion, while the replacement of Eu^{2+} with Gd^{3+} varies only the concentration of the conduction electron because the spin configuration of $Gd^{3+}(^8S_{7/2})$ is identical with that of Eu^{2+}. We can expect a continuous change in the exchange mechanism with changing the composition (x) in the solid solutions, $R_xEu_{1-x}C_2$ (R=La and Gd).

The magnetic data of the solid solutions, $R_xEu_{1-x}C_2$ (R=La and Gd), are tabulated in Tables 2 and 3, respectively. All the effective moments obtained from the χ_m^{-1} *vs.* T linear relation are in good agreement with the calculated values on the assumption that all the Eu ions in the compounds are bivalent. The solid solutions, $La_xEu_{1-x}C_2$, become ferromagnetic at low temperatures over the composition range from $x=0.08$ to $x=0.76$. The values of T_c(or θ_p) remain almost constant in the composition range from 0 to 0.47 and decrease rapidly with further dilution. In

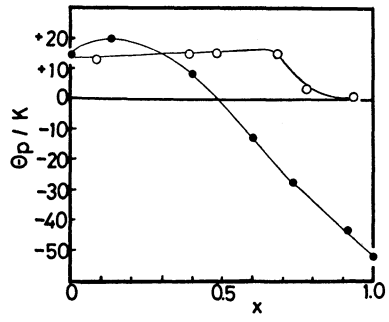

Fig. 4. Paramagnetic Curie temperature (θ_p) as a function of composition (x) for the solid solutions, $La_xEu_{1-x}C_2$ (—○—) and $Gd_xEu_{1-x}C_2$ (—●—).

the solid solutions, $Gd_xEu_{1-x}C_2$, the kind of magnetic order varies from ferromagnetic to antiferromagnetic with increasing the concentration of the Gd^{3+} ion. The composition dependence of θ_p for $R_xEu_{1-x}C_2$ (R=La and Gd) is shown in Fig. 4.

The carbides, $R_xEu_{1-x}C_2$, differ from the Eu chalcogenides such as $R_xEu_{1-x}Se$[23] in the magnetic behavior for small values of x ($x<0.1$). The compounds, $R_xEu_{1-x}Se$, have a drastic increase in θ_p and T_c for very low concentration of dopant (R=La^{3+} or Gd^{3+}) and this behavior was explained theoretically by Kasuya[24,25] in terms of the magnetic impurity model as follows. An excess electron with spin $\vec{s}_i$, which is trapped by a tervalent ion, magnetically polarizes the nearest neighbouring Eu spin, $\vec{S}_n$, by means of a strong exchange interaction between the impurity electron and the 4f electrons (the i-f exchange interaction). The large increase of T_c, ΔT_c, is deduced from the additional i-f exchange interaction, $-2\sum J_{in}\vec{s}_i\cdot\vec{S}_n$, and given by

$$k_B\Delta T_c = 2\sum J_{in}\vec{s}_i\cdot\vec{S}_n. \quad (1)$$

The Eu chalcogenides have a 6s character on the impurity state,[25] while the Eu dicarbides are expected to have a 5d character on the impurity state.[1,26] The almost constant T_c values of the solid solutions, $R_xEu_{1-x}C_2$, for the small values of x seem to be understood in the light of the small special spread of the impurity electron which would suppress the i-f exchange interaction. The magnetic behaviors of $R_xEu_{1-x}C_2$ for higher values of x resemble those of the Eu chalcogenides[23] and would be explained in terms of the change of Ruderman-Kittel function given by[27]

$$F(2k_FR) = [2k_FR\cos(2k_FR) - \sin(2k_FR)](2k_FR)^{-4}, \quad (2)$$

$$k_F = 1/r_0(9\pi z/4)^{1/3}, \quad (3)$$

where R is the distance from the magnetic ion of the reference site, k_F the Fermi wavenumber, r_0 the atomic radius, and z the number of conduction electrons.

Electrical Properties. Electrical resistivities of EuC_2 (ρ) decrease with decreasing temperature down to 160 K, and has a sharp peak at T_p=20 K as shown in Fig. 5. Inset is the ρ *vs.* T curves at various external fields (H). As the H values increase, the peak in ρ decreases, becomes broader, and shifts to higher temperature side. The T_p values exhibit the same

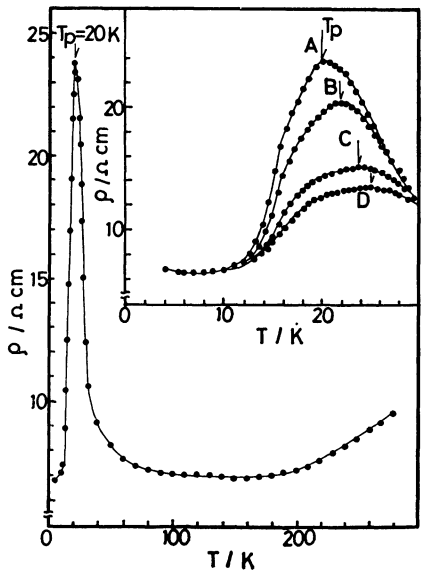

Fig. 5. Electrical resistivity (ρ) *vs.* temperature curve for EuC_2. Inset; the ρ *vs.* T curves at various fields (A: 0 kOe, B: 2.80 kOe, C: 5.60 kOe, D: 6.85 kOe).

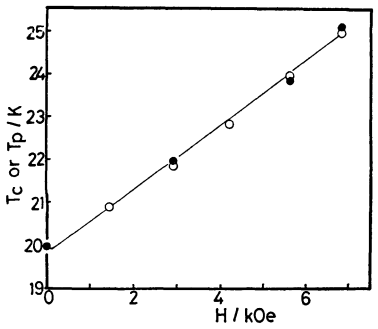

Fig. 6. Magnetic field (H) dependence of the Curie temperature (T_c, —○—) and the temperature at which the resistivity has the peak (T_p, —●—) for EuC_2.

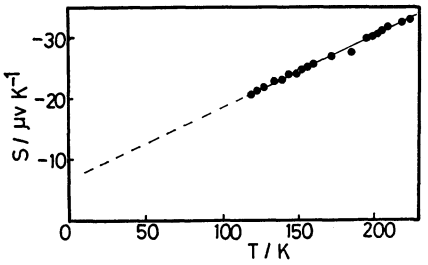

Fig. 7. Temperature dependence of the thermoelectric power (S) for EuC_2.

field dependence as the Curie temperatures (Fig. 6). The temperature dependence of the thermoelectric power (S) in EuC_2 is shown in Fig. 7. The sign of the S values is negative over the whole range of temperatures, indicating electron-type conduction. The creation of the excess electron in EuC_2 may be due to the existence of anion (C_2^{2-}) vacancies in small amount.

The rapid increase in ρ near the Curie temperature was observed previously for the Eu chal-

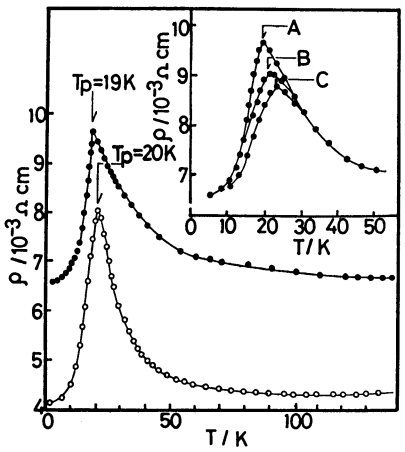

Fig. 8. Electrical resistivity (ρ) *vs.* temperature (T) curves for $La_{0.39}Eu_{0.61}C_2$ (—●—) and $Gd_{0.13}Eu_{0.87}C_2$ (—○—). Inset; the ρ *vs.* T curves at various magnetic fields (A: 0 kOe, B: 3.50 kOe, C: 6.85 kOe) for $La_{0.39}Eu_{0.61}C_2$.

cogenides.[28] Kasuya ascribed this electrical behavior to the exchange interaction between the impurity electron and the 4f electrons.[24,25] The impurity electron aligns the spins of nearest neighbour Eu^{2+} ions throughout the i-f exchange interaction, forming magnetic polarons. Therefore, the mobility of the impurity electron decreases near T_c. Since below T_c all the 4f spins are aligned and the magnetic polarons disappear, the resistivities decrease rapidly. When a magnetic field is applied, an activation energy which is necessary for hopping of the impurity electron is reduced and the peak in ρ decreases.

The electrical resistivity of $La_{0.39}Eu_{0.61}C_2$ or $Gd_{0.13}Eu_{0.87}C_2$, decreases to 1/1000 of that of EuC_2, reflecting the increase of conduction electron density (Fig. 8). A peak in ρ *vs.* T curve is similar to that observed for EuC_2 and would be explained on the basis of the same model as described above.

This work was supported by a Grant-in-Aid for Scientific Research No. 455301 from the Ministry of Education, Science and Culture for one of the authors (G. Adachi).

References

1) M. Atoji, *J. Phys. Soc. Jpn. Suppl.*, B-II **17**, 395 (1962).
2) R. E. Gebelt and H. A. Eick, *Inorg. Chem.*, **3**, 335 (1961).
3) P. Wachter, "Handbook on the Physics and Chemistry of Rare-Earths," ed by K. A. Gschneidner, Jr., and L. R. Eyring, North Holland, New York (1979), Vol. 2, p. 507.
4) G. Adachi, K. Ueno, and J. Shiokawa, *J. Less-Common Met.*, **37**, 313 (1974).
5) G. Adachi, H. Kotani, N. Yoshida, and J. Shiokawa, *J. Less-Common Met.*, **22**, 517 (1970).
6) G. Adachi, T. Nishihata, and J. Shiokawa, *J. Less-Common Met.*, **32**, 301 (1973).
7) I. J. McColm, T. A. Quigley, and N. J. Clark, *J. Inorg. Nucl. Chem.*, **35**, 1931 (1973).
8) M. A. Bredig, *J. Phys. Chem.*, **46**, 801 (1942).
9) T. C. Wallace, N. H. Krikorian, and P. L. Stone, *J. Electrochem. Soc.*, **111**, 1404 (1964).
10) A. L. Bowman, N. H. Krikorian, G. P. Arnold, T. C. Wallace, and N. G. Nereson, U.S.A. Energy Comm. LA-DC-8451 CESTI, **1967**, 7.
11) I. J. McColm, I. Colquhoun, and N. J. Clark, *J. Inorg. Nucl. Chem.*, **34**, 3809 (1972).
12) W. B. Wilson, *J. Am. Ceram. Soc.*, **43**, 77 (1960).
13) G. Adachi, Y. Shibata, K. Ueno, and J. Shiokawa, *J. Inorg. Nucl. Chem.*, **38**, 1023 (1976).
14) G. Adachi, F. Tonomura, Y. Shibata, and J. Shiokawa, *J. Inorg. Nucl. Chem.*, **40**, 489 (1978).
15) R. D. Shannon, *Acta Crystallogr., Sect. A*, **32**, 751 (1976).
16) M. Atoji and R. C. Medrud, *J. Chem. Phys.*, **31**, 332 (1959).
17) M. Atoji, *J. Chem. Phys.*, **35**, 1950 (1961).
18) R. M. Bozorth, "Ferromagnetism," D. Van Nostrand, New York (1951), p. 713.
19) T. Kasuya, *IBM J. Res. Develop.*, **14**, 214 (1970).
20) M. Atoji, *J. Chem. Phys.*, **46**, 1891 (1967); **48**, 3384 (1968); **52**, 6430 (1970); **57**, 2410 (1972).
21) T. Sakai, G. Adachi, and J. Shiokawa, *J. Appl. Phys.*, **50**, 3592 (1979).
22) T. Sakai, G. Adachi, T. Yoshida, and J. Shiokawa, *J. Less-Common Met.*, **81**, 91 (1981).
23) H. Holtzberg, T. R. McGuire, S. Methfessel, and J. C. Suits, *Phys. Rev. Lett.*, **13**, 18 (1964).
24) A. Yanase and T. Kasuya, *J. Appl. Phys.*, **39**, 430 (1968).
25) A. Yanase and T. Kasuya, *J. Phys. Soc. Jpn.*, **25**, 1025 (1968).
26) V. L. Yupko, G. N. Makarenko, and Yu. B. Paderno, "Refractory Carbides," ed by G. V. Samsonov, Consultants Burean, New York (1974), p. 251.
27) B. Coqblin, "The Electronic Structure of Rare-Earth Metals and Alloys: The Magnetic Heavy Rare-Earths," Academic Press, New York (1977).
28) Y. Shapira, S. Foner, and T. B. Reed, *Phys. Rev. B*, **8**, 2299 (1973).